Coupled Electromagnetic Field Computation with External Circuit for the Evaluation the Performance of Electric Motor Designs

A. Sarikhani and O. A. Mohammed

Energy Systems Research Laboratory
Department of Electrical and Computer Engineering
Florida International University, Miami, FL 33174, USA
mohammed@.fiu.edu

Abstract **--** In this paper, a set of PM machine's designs, having the similar level of nominal input and outputs i.e. voltage, torque, and speed were compared to evaluate the effectiveness of a computational design procedure. The designs include the machines with distributed winding arrangements, different number of slots, different pole widths, and different slot opening shapes. The physical characteristics of machines such as the cogging torque, back emf, flux linkages, and inductances were calculated from a 2D nonlinear transient finite element analysis with motion. The torque and speed profiles of all of the machines were calculated from the phase variable modeling approach. The phase variable model is a database representation of the machine's numerical model and it allows computationally efficient dynamic simulation of the coupled problem with realistic physics-based design. The phase variable models of the machines were linked to the driving circuit to determine the mutual effect of machine design parameter and the drive topology on the performance measures of machines.

Index terms-- Cogging torque, electromagnetic field computation, finite element analysis, motor design, phase variable model, PM machines.

I. INTRODUCTION

Electric machines play an essential role in many industries. PM synchronous motors are widely utilized due to their high power density, low maintenance costs, and high efficiency. From a structural point of view, depending on the setting of the magnets on the rotor, the synchronous motors can be constructed by either burying the magnets within the rotor iron or by mounting them on the rotor surface. Most PM synchronous motors can be categorized into three general categories; surface mounted PM synchronous motors (SPM) which have their permanent magnets mounted on the surface of the rotor, inset PM synchronous motors in which the permanent magnets are inset or partially inset into the rotor, and interior PM synchronous motors which have the permanent magnets completely buried inside the rotor [1]. From machine winding point of view, concentrated windings versus distributed winding for PM motors are widely used because of the low manufacturing cost. Comparisons and quantitative analysis of these two types of windings for two motors with same stator were studied [2, 3]. Nevertheless, it is recognized that in the case of design of the PM motor, infinite number of combinations would result in acceptable outputs. Depending on such outputs and the planned application, different designs could be achieved.

One of the intrinsic characteristics of PM motors is the pulsating torque. This ripple torque is parasitic, and can produce acoustic noise, mechanical vibration, and other problems in electric machine drive systems such as increased iron losses and total harmonic distortion [4]. Therefore, the machine designer must consider these issues in the design process [4, 5]. The study of pulsating torque is important for the application of constant speed or high-precision position control, especially at low speed applications. The torque pulsations are due to the cogging torque and the electromagnetic torque ripple. Many techniques for mitigating the cogging torque were proposed in the literature [6-8]. Some of the methods manipulate the stator or rotor separately or both of them together. This includes employing a fractional number of slots per pole, skewing of the magnets, slots, and/or the opening of slots, shifting and shaping of the main magnets, shifting the slots opening, optimizing the magnet pole-arc to

Submitted On: April 24, 2011
Accepted On: September 25, 2011

pole-pitch ratio, and introducing supplementary slots or teeth [6, 7, 8]. The fractional number of slots/pole can change both the amplitude and the frequency of the cogging torque to a desirable value. It also increases the fundamental order of the magnetic flux density in the air gap due to the different relative circumferential positions of the stator slots with respect to the edges of the magnets when this topology is used. On the other hand, the actual back emf waveform of PM motors depends on the conductor distributions and flux density. This in turn is a function of the magnetization characteristic of the magnet stator teeth, and slot structures.

PM machines with trapezoidal back emf have been widely used due to the simplicity in their control [9]. The skew of magnets is effective in reducing the harmonic content in the flux linkage and back EMF waveform, as well as in reducing the cogging torque [8].

As discussed above, different practical and theoretical methods have been proposed for mitigating the cogging torque, and also manipulating the back emf waveform for a simpler and cheaper driving strategy. In fact most of these strategies increase the cost because they alter the conventional manufacturing processes. In this paper, sets of designs representing studied cases were obtained from classic design procedure. Following this step, a finite element analysis was completed on each of the designed geometries. This was done to calculate the cogging torque, back emf, and flux linkage for all of the cases. Finally, a phase variable model was used to simulate the output torque and speed of the machine [11, 12]. The phase variable model is a data base table look up model of the nonlinear transient finite element solution of the motor to enable dynamic simulation.

II. CASE OF STUDIES

A. Preparation of case studies for field computation

The goal of this section is the preparation of a set of machines with different number of slots, pole widths, different slot opening shape, but with the same range of speed, input power, and voltage. Four different sets of machines were designed where the designs vary in the number of slots and pole widths. The totals of twenty one different machine designs were considered. A schematic view of the designed machine is shown in figures 1(a) and 1(b). All of the machine designs created from a classic design procedure [1, 10] for a WYn winding, 2-hp, 1200-rpm, 6-pole, phase voltage of 111.5-Volt, and current density of 3 A/mm^2.

The difference in the designs of the machines is shown in Table 1. In the first set, we have eighteen slots with four different pole widths which make four different machines, and all of the coils in the stator are in series together in each phase. In the second set, the number of slots were changed to thirty six, and four different poles width make four different machines, where there is two parallel paths for currents in each phase. The other sets were designed for fifty four and seventy two slots, respectively as shown in Table 1. In this table N_p, S_p, and C_s stand for number of parallel paths, number of slot per pole, and coil span, respectively. The design details for the various sets were illustrated in Tables 2 and 3. The used magnetic material for all of the machines is Sm2Co17. The magnets are radically magnetized. After a classic design procedure, each machine was prepared for an FE analysis as shown in Figure 2 (b). Here, the accuracy of manufacturing tolerance is assumed as 0.05 millimeter. Therefore all of the design parameters are rounded to the nearest real value.

Another test set was prepared where the influence of the slot opening geometry on the physical behavior of the machine and its performance measure was investigated. In order to examine the influence of the slot opening geometry, the five 36-slot/6-pole machine designs shown in Figure 1(c) were considered. The details of stator geometry are shown in Table 3. The inter pole angles in all of the designs were two degrees while the rotor geometry remain the same for these five test shown in Table 4. In this set of tests, Design 1 has tapered tooth tips and parallel slot opening. Design 2 has straight tooth tips and parallel slot opening, Design 3 has straight tooth tips and no slot opening, Design 4 has tapered tooth tips and non-parallel slot opening, and Design 5 has straight tooth tips and non-parallel slot opening. All the other stator design parameter remains the same for all of the designs. It is mentioned that, the chosen current density for this range of machine ensure us the thermal limitations; however for a secure and optimal design, a thermoelectric design procedure will be a superior solution.

Here, depending to the voltage value of the DC bus before the conventional 6-switch, 3-phase

DC/AC inverter and also control strategy of the inverter, the maximum amplitude of the back emf should be chosen otherwise the desired speed and torque characteristics will not be achieved. The four well-known, modulation strategies for the inverter connected to the motors are: six-step inverter control, sinusoidal PWM, space vector PWM, harmonic elimination, hysteresis, Delta and Third harmonic injections. The respective phase-neutral DC bus utilization of each of these control strategy are $2V_{dc}/\pi$,$V_{dc}/2$ with modulation factor equal to one, $V_{dc}/\sqrt{3}$, $2\,V_{dc}/\pi$, $V_{dc}/2$, $V_{dc}/2$, and $V_{dc}/\sqrt{3}$. The rule is that the maximum amplitude of the back emf voltage of each of the phases should be always lower than the phase-neutral voltage in order to ensure us a proper speed control. If this rule is ignored then unwanted fluctuations will appear in the torque and speed profiles and more probably the speed control will lost. Therefore, in this paper the number of coil's turns per phase is chosen based upon this criterion. In this work, the voltage of the DC bus for the inverter is chosen as 300-V, and the control strategy is chosen as Hysteresis current regulated control, therefore the maximum back emf voltage is limited to a value lower than 150-V. However, for a secure current hysteresis control for a wide speed range, the maximum back emf should be chosen with a good security margin. Here, it is assumed that the drive is not equipped with the flux weakening control therefore in the designs the maximum amplitude of the fundamental component of the back emf were limited to 100-V to offer more security margin for over speed conditions, likely 150% of the nominal speed. The hysteresis band in the hysteresis current control is fixed as 0.3 Ampere.

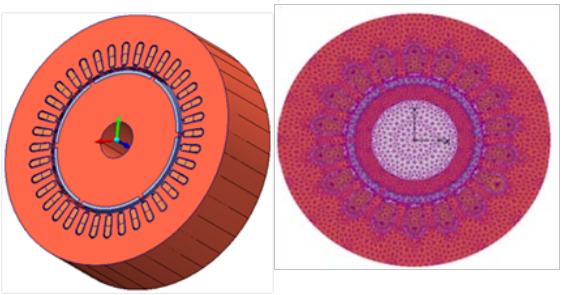

Fig. 1. (a) A schematic 2D view of the studied case.

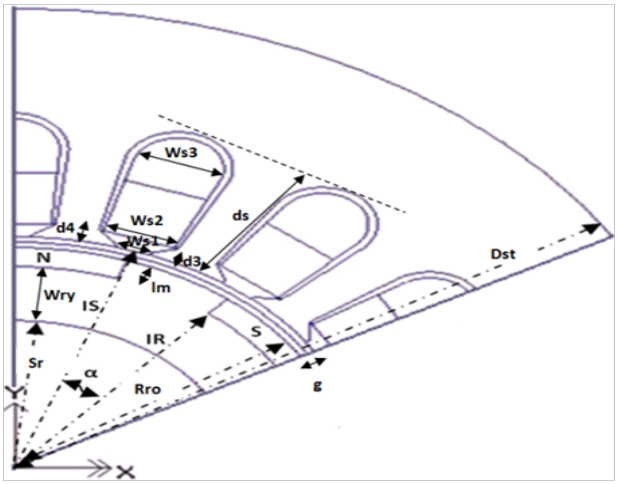

Fig. 1. (b) A schematic 2D view of the studied.

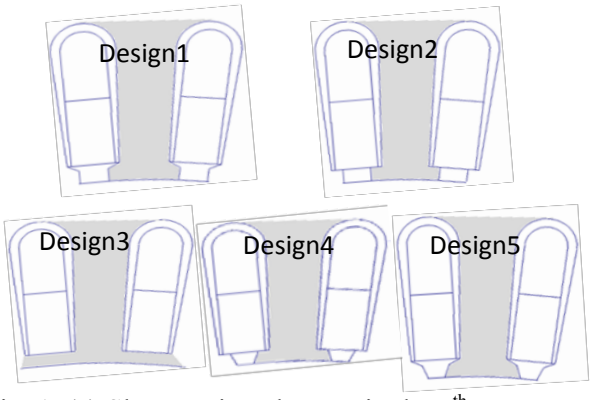

Fig. 1. (c) Slot opening changes in the 5th test set.

Table 1: Winding arrangements and inter pole angle of studied cases

(N_s)	Np	Slot/pole	Sp	Cs	α° (degree)	Coil/phase
18	1	3	60	3	(0°,2°,5°,10°)	17
36	2	6	30	5	(0°,2°,5°,10°)	17
54	3	9	20	8	(0°,2°,5°,10°)	17
72	4	12	15	10	(0°,2°,5°,10°)	17

Table 2: Stator geometry of 1th to 4th sets (in mm)

Set	N_s	W_{s3}	W_{s2}	W_{s1}	d_3	d_4	d_s	D_{st}	L_{st},
1st	18	22.2	16.8	7.4	3	0.8	37	138	50
2nd	36	11	8.4	3.6	3	0.8	37	138	50
3rd	54	5.6	4.2	1.8	3	0.8	37	138	50
4th	72	2.8	2.1	1	3	0.8	37	138	50

Table 3: Stator geometry of 5th set (in mm)

	Ns	W_{s3}	W_{s2}	W_{s1}	d_3	d_4	d_s	D_{st}	L_{st},
1	36	8.15	6.4	3.6	0.75	1.9	19.8	126.6	74.5
2	36	8.15	6.4	3.6	0	1.9	19.1	126.6	74.5
3	36	8.15	6.4	0	0	2.3	19.4	126.6	74.5
4	36	8.15	6.4	2.1	0.76	1.9	19.8	126.6	74.5
5	36	8.15	6.4	2.1	0	1.9	19.1	126.6	74.5

Table 4: Rotor geometry of studied case (mm)

Set number	Rro	Sr	Wry	Lm	g
All sets	66.6	44.1	16.4	5.8	3

III. THE PHASE VARIABLE MODEL

The phase variable model of PM machines is an accurate and fast model for the purpose of integrated drive system simulations. This model uses transient FE solutions to establish a detailed block description of the implemented machines in a Simulink environment as shown in Figure 2(a). This model accounts for flux weakening as well as other performances [11, 12, and 14]. The model is essentially a database representation of the nonlinear transient operation of the machine to allow the use of a detailed computational model for dynamic simulation.

The creation of the phase variable model consists of two discrete steps. In the first step, a linear transient FE analysis is performed to calculate the cogging torque, back emf, flux linkage, and the inductance matrix of the machine. The FE-based phase variable model is rotor –position dependent, therefore, the FE analysis must take the transient analysis and the motion of rotor into account. In the FE domain, the corresponding magnetic vector potential formulation is calculated as:

$$-\nabla.\left(\sigma\frac{\partial A}{\partial t}-\sigma\vartheta\times(\nabla\times A)-J^{e}\right)=0 \quad (1)$$

$$\sigma\frac{\partial A}{\partial t}+\nabla\times(\mu^{-1}\nabla\times A-M)-\sigma\vartheta\times(\nabla\times A)=J^{e} \quad (2)$$

where σ is the conductivity, A is the vector potential, ϑ is the velocity of the modeled object, J^{e} is the external current density, μ is the permeability, and M is the magnetisation. The constitutive relation considering ferromagnetic saturation is:

$$B=\mu_0(H+M) \quad (3)$$

where B is the flux density, H is the field strength, and μ_0 is the permeability of air.

Following the FE analysis, the FE output parameters are collected into lookup tables in the circuit environment. The second step is the implementation of the machine equations, equations (4) - (8), in the circuit environment. The values are retrieved via look-up tables to create the database and implement it. In the circuit environment, the back emf, and the flux linkage, cogging torque as well as the Inductances are updated for each rotation position varying with the speed of the machine. Rotor-position-dependent inductance matrix is calculated by the incremental method [13]. Following the implementation of the phase variable model in Simulink, a hysteresis current regulated drive with speed controller were linked with the phase variable model of the machine to control the speed as given in Figure 2 (b).

$$V_{abc}=R_{abc}i_{abc}+{}^{d\varphi_{abc}(i_{abc},\theta)}/_{dt} \quad (4)$$

$$\varphi_{abc}(i_{abc},\theta)=\varphi_{sabc}(\theta)+\varphi_{rabc}(\theta)=L_{abc}(\theta)i_{abc}+\varphi_{rabc}(\theta) \quad (5)$$

$$T_M=[p(0.5i_{abc}^{T}dL_{abc}(\theta)/d\theta).i_{abc}+i_{abc}^{T}d\varphi_{rabc}(\theta)/d\theta]+T_{cog}(\theta) \quad (6)$$

$$\frac{Jd\omega}{dt}=T_m-F\omega-T_L \quad (7)$$

$$\omega=d\theta/dt \quad (8)$$

In the above equations, V_{abc}, $R_{abc,}$ and i_{abc} are the terminal voltage, resistance, and current of the stator winding, respectively. The flux linkage φ_{abc} is composed of two parts, see Eq. (5). The first part is related to the inductance L_{abc} of the stator winding, while the other part is contributed by the permanent magnets on the rotor, represented by φ_{abc}. The cogging torque T_{cog} is added to obtain the total output torque T_m, as shown in Eq. (7). The rotation angle of the rotor position is represented by θ. Here, L_{abc}, φ_{abc} and T_{cog} are considered as rotor-position-dependent parameters. Also, in these equations p, J, ω and F are the number of pole pairs, inertia, angular speed, and friction factor, respectively. The load torque is T_L in Eq. (7).

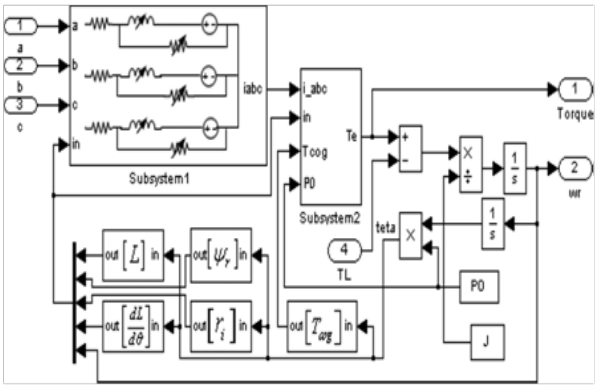

Fig. 2. (a) Phase-variable model of PM machine [14].

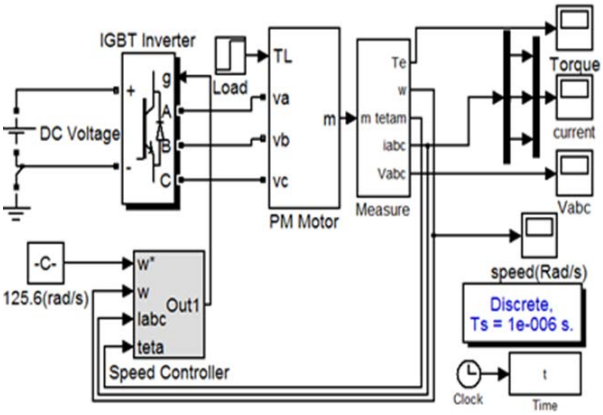

Fig. 2. (b) Phase variable model with hysteresis IGBT driver and speed controller.

IV. SIMULATION RESULTS

A. The cogging torque

The cogging torque is the consequence of the interaction between the permanent magnet fields and the stator in the neighbor of the air gap that is because of the reluctance variations with the rotor position and that is independent of the stator current [11]. Figure 3 (A) to (D) show the simulated cogging torque for different angle α. It can be observed that the maximum value of cogging torque and its frequency is dependent to the number of slots and pole widths. In this study, as α is changed, the inner radius of the poles are kept unchanged. From Figure 3, it is concluded that for the eight slots and by decreasing the pole width, the maximum of the cogging torque is reduced, but its frequency increases. Therefore, it is concluded that a change in the angle α would change the cogging torque to a better value. As can be seen in Figures 3 (a) to (d), it is concluded that the cogging torque can be a function of (α, Ns) which has a minimum that, in this case, occur at α=2 degree. Moreover, by comparison of Figures 3 (a) to (d), it is concluded that the number of slots in the design procedure would highly have an influence on the maximum amplitude of the cogging torque.

The cogging torque calculation in the 5th set, Figure 3 (e), shows that the 2nd design has the highest cogging torque and the 3th design has the lowest cogging torque. The cogging torques of the 1st, 4th, and 5th designs are almost similar with the maximum amplitude equal to 0.6 (n. m).

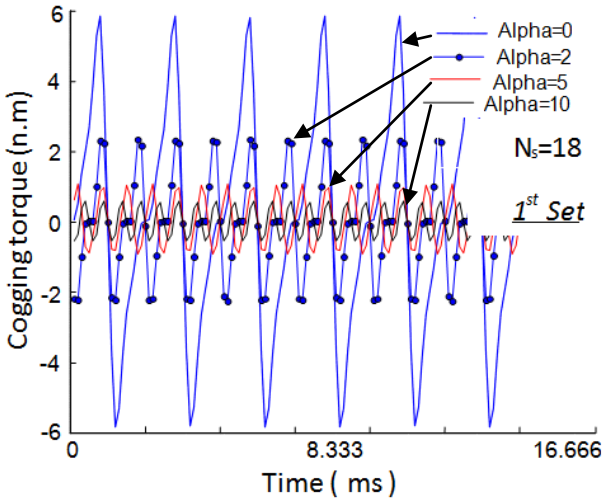

Fig. 3. (a) Cogging torque of the 1st set.

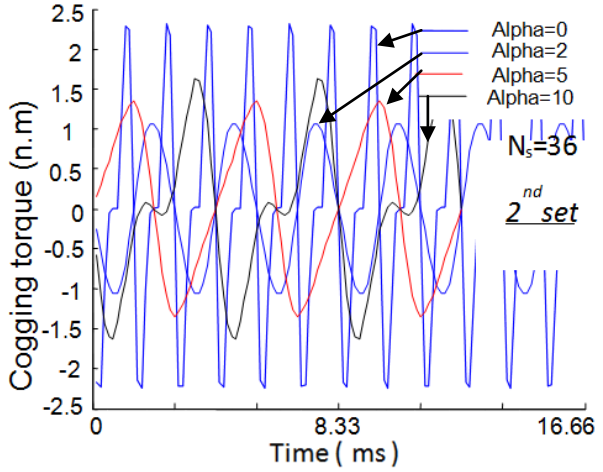

Fig. 3. (b) Cogging torque of the 2nd set.

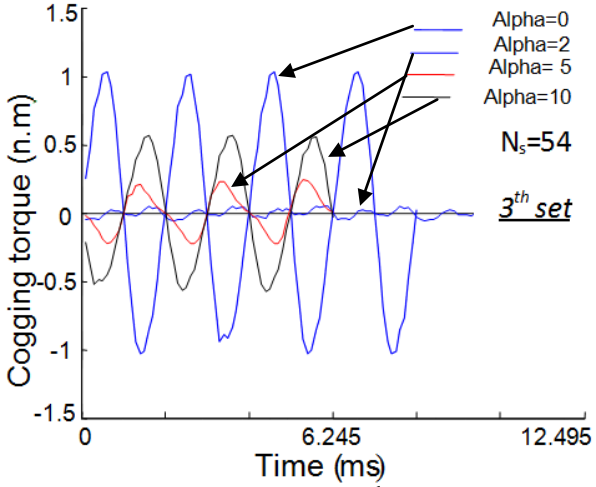

Fig. 3. (c) Cogging torque of the 3th set.

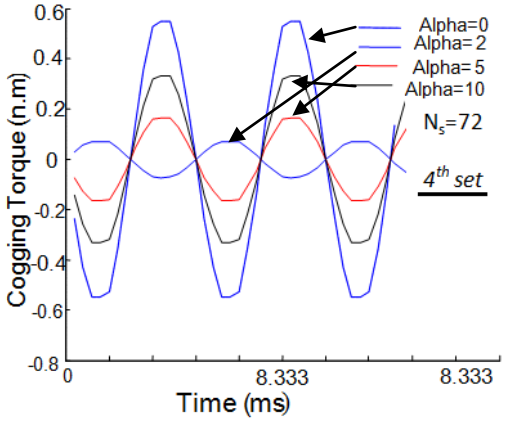

Fig. 3. (d) Cogging torque of the 4th set.

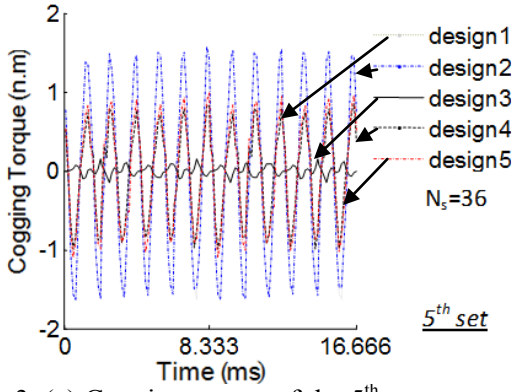

Fig. 3. (e) Cogging torque of the 5th set.

B. The back emf and flux linkage as a function of design parameters:

The back emf is the consequence of the induced voltage in the coils due to the rotation of the magnetic field produced by the magnets. The waveform of the back emf has a direct influence on the machine current and therefore the torque ripple [11-12]. As can be seen from Figure 4, as the pole width is decreased, i.e. when α is increased, the flux opens a new path through the iron of the inter-pole to the rotor yoke. Therefore, the concentration of flux inside the coils is decreased and therefore the root mean square value of the induced back emf in the coils is reduced.

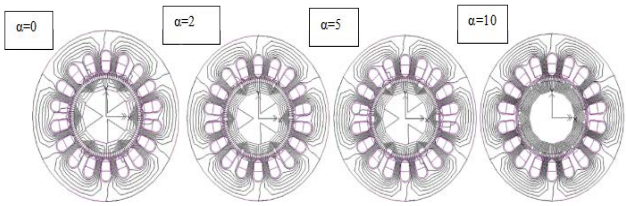

Fig. 4. The flux picture as a function for the 1th set.

Figures 5 (a) to 5 (d) show the back emfs for different pole width and number of slots. As can be seen from these figures, when the number of slots is increased the influence of the pole width becomes more visible. For example, for 72 stator slots, as the angle α increase, the back emf waveforms become more similar to a sinusoidal waveform than for the 36 slots machine. Also one can observe that the maximum value of the back emf is independent of the angle α. Therefore, it is concluded that the back emf of a motor with a higher number of slots is more sensitive to the pole width. In fact the shape of the back emf has an essential role for choosing the driving strategy. By comparison of Figures 8(a) to (d) it can be concluded that, if a trapezoidal waveform of the back emf is required, the lower inter-pole angle is preferable and if a sine waveform of the back emf is required, a higher inter-pole angle would be preferable although this conclusions is almost validated for radial and parallel magnetized permanent magnets with equal inter-pole angles [1]. Moreover, by comparison of the Figures 5(a) to (d) concerning different number of slots it is seen that the machines with higher number of slots can provide the drive circuit with better trapezoidal or sine back emf waveform; for example, in Figure 5 (a) it is seen that achievement of a pure sine or a pure trapezoidal back emf waveform is indeed unachievable. In fact, creation of a proper current for ripple free performance with the used drive topology and winding arrangement maybe not be feasible.

On the other hand, a closer look at the effect of the number of slots reveals that with smaller number of slots, a smaller number of coils are required. However, the number of turns per coil and the size of the slot would be larger. A small number of slots may lead to a small savings in cost. However, the effect of the stator slots on the air gap flux and therefore back emf in small machines is considerable.

Figure 6 (a) show the flux linkage of the 1st to 4th set. As can be seen from this Figure, the number of slots has minor influence on the maximum amplitude of flux linkage, but as the pole width is decreased the maximum amplitude of the flux is decreased. Moreover, the flux linkage of the 5th set, Figure 6 (b), shows that, the 3rd set has the lowest flux linkage that the reason is that the flux closes its path in the added iron to the slot openings area. The flux linkages of other test set are relatively

remained unchanged.

Figures 7 (a) and 7 (b) show the self and mutual inductances of the 5th set. As it is seen from the inductance profiles, the 3rd design has the highest self and the lowest mutual inductance. The self and the mutual inductance of the other designs are at the same level. It is evident that the slot opening geometry has a noticeable effect on the inductances. This shows that, the machines with the highest inductances have higher start-up time but have lowest speed fluctuations. Moreover, the inductance study of the 1th to 4th set show that, the higher number of slot/pole ratio, the lower will be the winding inductance ratio. This is due to the number of the series turns per phase reduces in order to achieve a given back emf.

Figures 8(a) and 8 (b) show the total output torque against different number of slots and slot openings shapes respectively. The output torque is obtained from simulation of the phase variable model. All of the simulations had the same drive system. A hysteresis band speed controller was used to control the speed. The torque is calculated for the pole width in which the cogging torque has minimum values in all of the cases, i.e. the value of α is equal to 2. As illustrated in Figure 8 (a), as the number of slots is increased, the torque ripples and the setting time of the torque is decreased. In figure 8 (b) less torque ripple compared to other designs is seen.

Figures 9(a) and 9(b) show the speed profile with different number of slots and slot openings shapes, respectively. From Figure 9 (a), it is concluded that the higher number of slots has lower speed fluctuations which can be an important factor for some special application. In Figure 9 (b), design 3, lower speed fluctuation but higher start-up time compared to other machines is seen. The hysteresis current loop control used for the speed control of the machine has higher dynamic comparing to other modulation strategies such as SVPWM, SPWM, harmonic elimination, etc. This method is also sensitive to the inductance of the electrical load. As the inductance of the machine is increased the current ripple is decreased. As a result, the electrical torque ripple and the speed fluctuations is decreased. However, the higher inductance the start-up time of the machine and the setting time of the speed during start-up or any change in speed reference is increased.

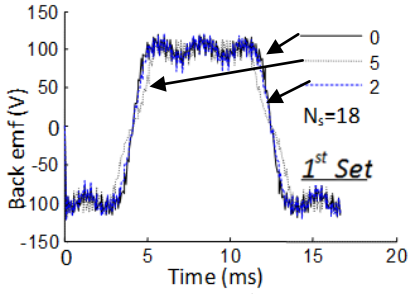

Fig. 5. (a) Back emf of the 1st set.

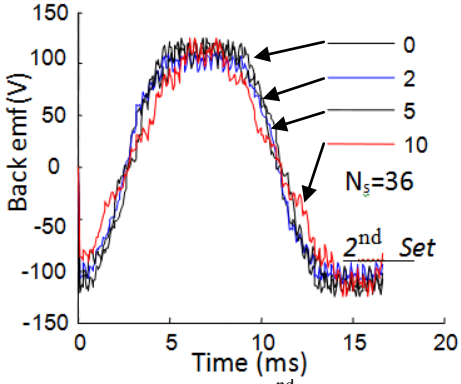

Fig. 5. (b) Back emfs of the 2nd set.

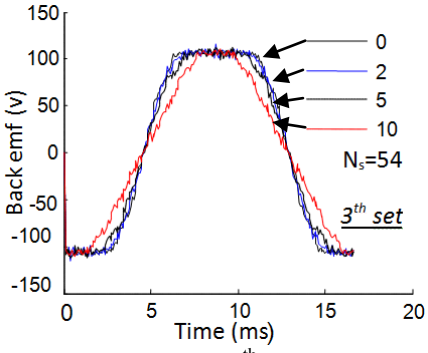

Fig. 5. (c) Back emfs of the 3th set.

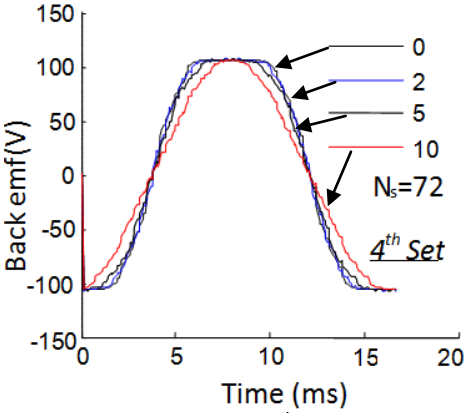

Fig. 5. (d) Back emfs of the 4th set.

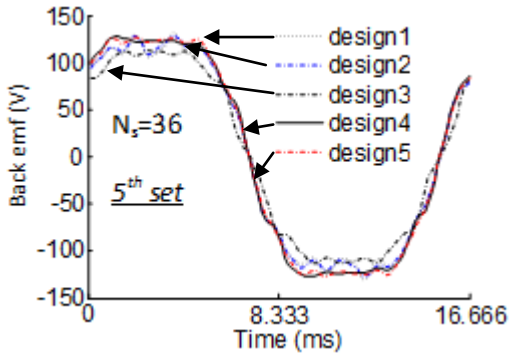

Fig. 5. (e) Back emfs of the 5th set.

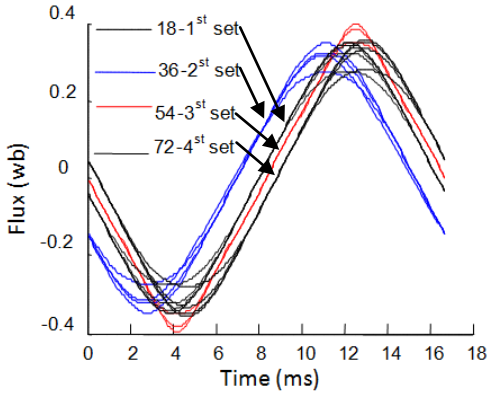

Fig. 6. (a) Flux linkage of the 1st to 4th set.

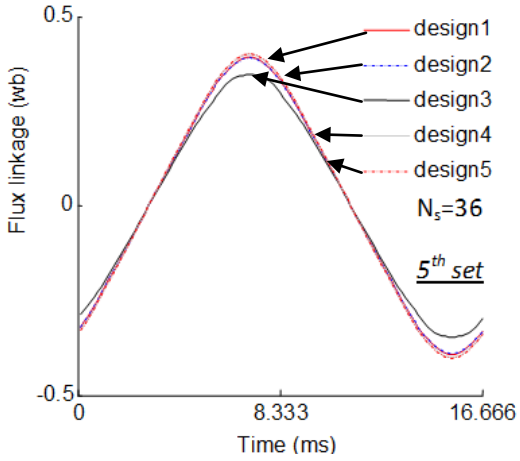

Fig. 6. (b) Flux linkage of the 5th set.

V. CONCLUSION

We investigated the effect of the number of slots, pole width, and slot openings shape as design parameters on the cogging torque, back emf, flux linkage, total torque, and speed for various PM motors controlled by a sinusoidal current regulated drive. The study was performed on twenty one different machines with similar nominal range of inputs/output. The simulation results shown that as the number of slots was increased, the cogging torque was generally decreased. In addition, it was shown that the pole width has a good potential to effectively change the cogging torque. It was found that a minimum cogging torque can be found for a specific pole width. Moreover, it was shown that a machine with higher number of slots has lower setting time compared to a machine with lower number of slots where the speed fluctuations and torque ripples were also relatively reduced. It can be concluded that a machine with higher number of slots can show better performance measures than a machine with lower number of slots, although it may increase the cost and require more accuracy in manufacturing tolerances.

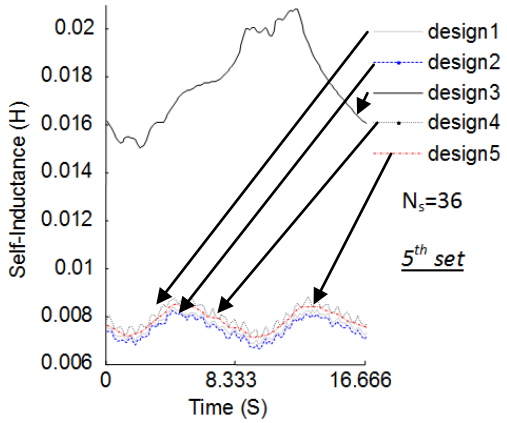

Fig. 7. (a) Self-inductances of the 5th set.

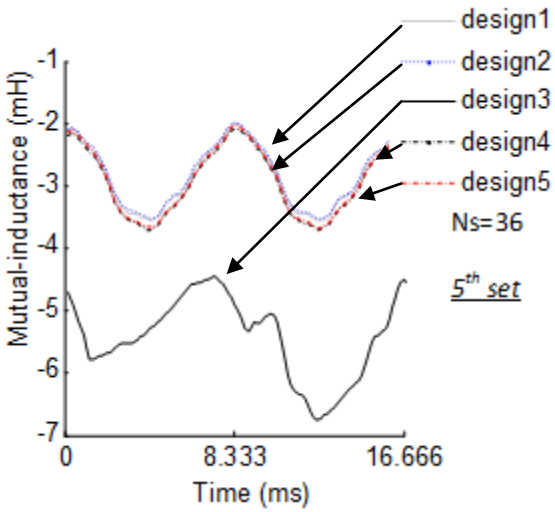

Fig. 7. (b) Mutual inductances of the 5th set.

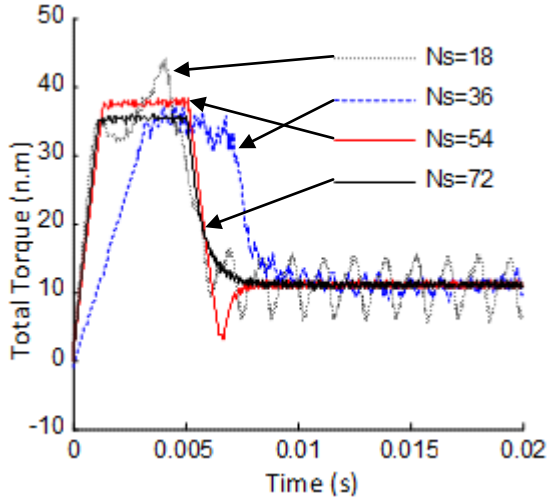

Fig. 8. (a) Total torque for α equal to 2 degree concerning different number of slots.

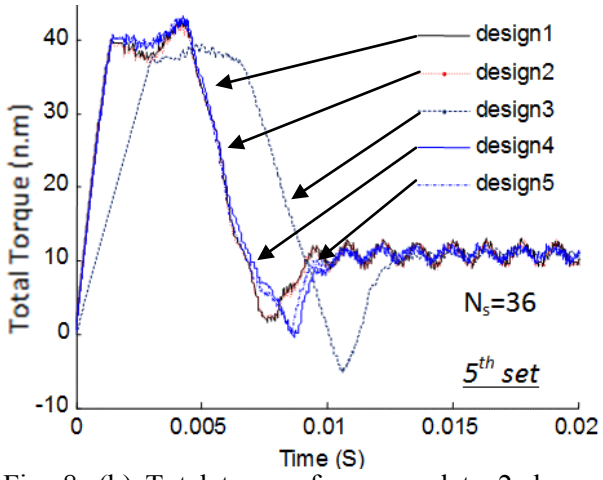

Fig. 8. (b) Total torque for α equal to 2 degree concerning different slot opening shape.

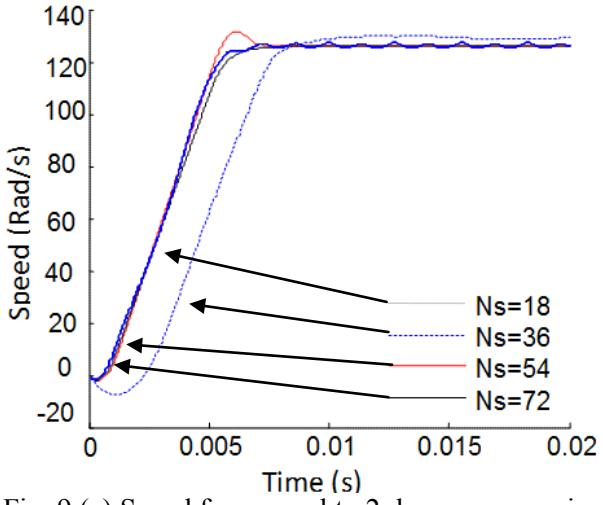

Fig. 9 (a) Speed for α equal to 2 degree concerning different number of slots.

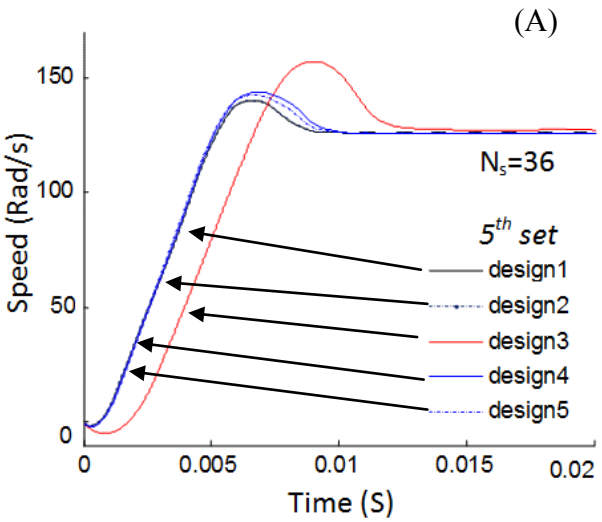

Fig. 9. (b) Speed for α equal to 2 degree concerning different slot opening shape.

ACKNOWLEDGMENTS

Part of this work is supported by a grant from the Office of Naval Research.

REFERENCES

[1] Duan Hanselman, *Brushless Permanent Magnet Motor Design*, Manga Physics, pp. 68-160 and 352-360, March 2003.

[2] F. Magnussen, P. Thelin, and C. Sadarangani, "Performance Evaluation of Permanent Magnet Synchronous Machines with Concentrated and Distributed Windings Including the Effect of Field-Weakening," *2nd IEE Inter. Conf. on Power Elec., Machines and Drives*, Edinburgh, UK, vol. 2, pp. 679-85, 2004.

[3] M. El-Refaie, T. M. Jahns, and D. W. Novotny, "Analysis of Surface Permanent Magnet Machines with Fractional-Slot Concentrated Windings," *IEEE Trans. Energy Conversion*, vol. 21, no. 1, pp. 34-43, Mar. 2006.

[4] L. Dosiek and P. Pillay, "Cogging Torque Reduction in Permanent Magnet Machines," *IEEE trans. on Industry application*, vol. 43, no. 6, pp. 1656–1571, 2007.

[5] Z. Q. Zhu and D. Howe, "Influence of Design Parameters on Cogging Torque in Permanent Magnet Machines," *IEEE Trans. Energy Conversion*, vol. 15, no. 4, pp. 407-412, 2000.

[6] Z. Q. Zhu, S. Ruangsinchaiwanich, and D. Howe, "Synthesis of Cogging Torque Waveform form Analysis of a Single Stator Slot," *IEEE Trans Industry App.*, vol. 42, no. 3, pp. 650-657, 2006.

[7] P. Salminen, J. Pyrhönen, F. Libert, and J. Soulard, "Torque Ripple of Permanent Magnet Machines with Concentrated Windings," ISEF *International*

Symposium on Electromagnetic Fields in Mechatronics, Electrical and Electronic Engineering, Baiona, Spain, 2005.

[8] S. A. Saied and K. Abbaszadeh "Cogging Torque Reduction in Brushless DC Motors Using Slot-Opening Shift," *Advances in Electrical and Computer Engineering*, vol. 9, no. 1, 2009.

[9] S. Tomy and G. Vineeta, "Analysis of Induced EMF Waveforms and Torque Ripple in a Brushless Permanent Magnet Machine," *IEEE Trans. On Indr. App*., vol. 32, no. 1, January 1996.

[10] M. G. Say, "Performance and Design of AC Machines," 3ed. 1958.

[11] O. A. Mohammed, Z. Liu, and S. Liu, "Stator Power Factor Adjustable Direct Torque Control of Doubly-Fed Induction Machines," Proceedings of the *International Electric Machines and Drives Conference IEMDC'05*, pp. 572-578, May 2005.

[12] O. A. Mohammed, S. Liu, and Z. Liu, "A Phase Variable Model of Brushless DC Motor Based on Physical FE Model and its Coupling with External Circuits," *IEEE Transactions on Magnetics*, vol. 41, no. 5, pp. 1576-1579, May 2005.

[13] M. Gyimesi and D. Ostergaard, "Inductance Computation by Incremental Finite Element Analysis," *IEEE Trans. On Magnetics*, vol. 35, pp. 1119-1122, May 1999.

[14] S. Liu, O. A. Mohammed, and Z. Liu, "An Improved FE-Based Phase Variable Model of PM Synchronous Machines Including Dynamic Core Losses," *IEEE Trans. On Magnetics*, vol. 43, no. 4, April 2007.

Ali Sarikhani started his bachelor in Transmission and Distribution Engineering in Power and Water University of Technology, Iran. He followed his Master in Power Electrical Engineering in Shahrood University of Technology, Iran. He is now a Ph.D. candidate of electrical engineering at Energy Systems Research Laboratory, Florida International University, USA. His current interests are the computational design prototyping, design adaptation and fault diagnosis of electrical apparatus by standard and intelligent systems.

Osama A. Mohammed (S'79, SM'84, F'94) is a Professor of Electrical and Computer Engineering and the Director of the Energy Systems Research Laboratory at Florida International University. He received his M.S. and Ph.D. degrees in Electrical Engineering from Virginia Polytechnic Institute and State University. He published numerous journal articles over the past 30 years in areas relating to power systems, electric machines and drives, computational electromagnetics and in design optimization of electromagnetic devices, artificial intelligence applications to energy systems. He authored and co-authored more than 300 technical papers in the archival literature. He has conducted research work for government and research laboratories in shipboard power conversion systems and integrated motor drives. He is also interested in the application communication and wide area networks for the distributed control of smart power grids. He has been successful in obtaining a number of research contracts and grants from industries and Federal government agencies for projects related to these areas. Professor Mohammed also published several book chapters including; Chapter 8 on direct current machinery in the Standard Handbook for Electrical Engineers, 15th Edition, McGraw-Hill, 2007 and a book Chapter entitled " Optimal Design of Magnetostatic Devices: the genetic Algorithm Approach and System Optimization Strategies," in the Book entitled: Electromagnetic Optimization by Genetic Algorithms, John Wiley & Sons, 1999.

Professor Mohammed is a Fellow of IEEE and is the recipient of the IEEE PES 2010 Cyril Veinott Electromechanical Energy Conversion Award. Dr. Mohammed is also a Fellow of the Applied Computational Electromagnetic Society. He is Editor of IEEE Transactions on Energy Conversion, IEEE Transactions on Magnetics, Power Engineering Letters and also an Editor of COMPEL. Professor Mohammed is the past President of the Applied Computational Electromagnetic Society (ACES). He received many awards for excellence in research, teaching and service to the profession and has delivered numerous invited lectures at scientific organizations around the world.

Professor Mohammed has been the general chair of several international conferences including; ACES 2006, IEEE-CEFC 2006, IEEE-IEMDC 2009, IEEE-ISAP 1996 and COMPUMAG-1993. He has also chaired technical programs for other major international conferences including; IEEE-CEFC 2010, IEEE-CEFC-2000 and the 2004 IEEE Nanoscale Devices and System Integration. Dr. Mohammed also organized and taught many short courses on power systems, Electromagnetics and intelligent systems in the U.S.A and abroad. Professor Mohammed has served ACES in various capacities for many years. He also serves IEEE in various Boards, committees and working groups at the national and international levels.